SWU Engineering Journal (2015) 10(2), 19-27
วารสารวิศวกรรมศาสตร์ มหาวิทยาลัยศรีนครินทรวิโรฒ
ปีที่ 10 ฉบับที่ 2 เดือนกรกฎาคม – ธันวาคม พ.ศ. 2558

Photocatalytic and Antibacterial Activities of TiO_2 Powder Synthesized by Microwave-assisted sol-gel Method

Weerachai Sangchay[1]* Mathana Khanghamano[2] and Kornkanok Ubolchollakhat[3]
[1]Faculty of Industrial Technology, Songkhla Rajabhat University, Songkhla 90000, Thailand
[2]Faculty of Engineering, Prince of Songkla University, Songkhla 90112, Thailand
[3]Faculty of Science, Thaksin University, Pattalung 93110, Thailand
*Corresponding author: Email: weerachai.sang@yahoo.com

ABSTRACT

TiO_2 powder was prepared by microwave-assisted sol-gel method. The powder was refluxed at 180 W for 1, 2 and 3 h and dried at 180 W for 1 h by a conventional microwave oven. Several analytical techniques including X-ray diffraction (XRD), scanning electron microscopy (SEM) and surface area measurement (BET) were employed to characterize the synthesized powder. Photocatalytic activity of the powder was also examined via the degradation of methylene blue (MB) solution under UV irradiation for a certain time. The efficiency of antibacterial activity was evaluated by the inactivation of *Escherichia coli* (*E.coli*). The results showed that only anatase TiO_2 was observed and the as-prepared powder exhibited the agglomeration of spherical nanoparticles with crystallite sizes of 20.7, 13.8 and 9.3 nm when the refluxed time was 1, 2 and 3 h, respectively. The highest efficiency for the photocatalytic and antibacterial activities was 66.68 and 100.00%, respectively, belonging to those powders using the refluxed time of 3 h.

Keyword: TiO_2 powder, Photocatalytic activity, Antibacterial activity, Microwave-assisted

1. Introduction

In recent years, titanium dioxide (TiO_2) is used for a wide range of applications such as photocatalyst, self-cleaning surfaces, solar cells, water and air purification, gas sensing and optical coating [1-3] because of its unique properties including good photocatalytic activity, chemical stability, non toxic nature, large band gap and low cost [4-6]. TiO_2 has three different crystal structures: anatase, rutile and brookite [7-9]. Anatase and rutile phases possess superior photocatalytic activity to the brookite one [10-11] and hence they are good candidates for photocatalysis applications.

Many efforts have been carried out to modify morphology and phase structure of TiO_2 powder using various methods such as hydrothermal synthesis, sol-gel, anodization, template and microwave-assisted [12-14]. However, the conventional sol-gel method usually suffers from high processing temperature and long reaction time, leading to grain growth and phase transition [15]. It is therefore necessary to consider an alternative technique to overcome those drawbacks. In the last few years, microwave

irradiation has been reported to effectively enhance the efficiency of sol-gel method on the preparation of inorganic materials. The microwave-assisted sol-gel method has unique advantages of uniform and rapid heating in comparison with the conventional one. In addition, this method can significantly reduce the processing time and simplify the preparation procedures as well as improve the nanometer size fraction of particles [16]. In addition, the method saves energy and appears today as a new technology for green chemistry development by means of solvent-free and/or less reactant needed. Recently, the microwave-assisted method has been used to synthesize different morphologies of TiO_2 powder [17].

In this study, a facile method for synthesizing TiO_2 powder via microwave-assisted sol-gel technique using titanium (IV) isopropoxide as a Ti precursor was developed. The prepared powder was refluxed at 180 W for 1, 2 and 3 h and dried at 180 W for 1 h by a conventional microwave oven. The physicochemical characteristics of the powder including crystallization, morphology and specific surface areas were characterized by X-ray diffraction (XRD), scanning electron microscopy (SEM) and surface area measurement (BET), respectively. The photocatalytic activity was also examined via the degradation of methylene blue (MB) solution under UV irradiation. Finally, antibacterial activity efficiency was evaluated by the inactivation of *Escherichia coli* (*E.coli*).

2. Experimental

2.1 Powders preparation

All chemicals used were of analytical research grade and employed without further purification and obtained from Fluka. Titanium (IV) isopropoxide ($Ti(OCH(CH_3)_2)_4$, TTIP, 97%) and hydrochloric acid (HCl, 97%) were used as a starting material and a peptizer, respectively [18]. TiO_2 powder was prepared via a conventional sol-gel method [19]. Firstly, to prepare TiO_2 sol, TTIP (10 ml), ethanol (150 ml) and water (250 ml) were mixed and stirred for 15 min at room temperature. The solution was acidified to pH = 3 by adding few droplets of 2 M HCl into the solution and stirred for 45 min. The treated solution was refluxed at 180 W for 1, 2 and 3 h using a domestic microwave oven (Samsung, ME82V) to produce a milky dispersion. The obtained solution was then dried using the microwave oven at 180 W for 1 h to receive TiO_2 powder. The powder product, however, was agglomerated and so grinding process was further required to reduce the agglomeration. In this work, TiO_2 powder refluxed at 180 W for 1, 2 and 3 h was designated as T1, T2 and T3, respectively.

2.2 Powders characterizations

Morphology and particle size of the synthesized TiO_2 powder were characterized by scanning electron microscope (SEM) (Quanta 400). Specific surface area of the powder was analyzed using quanta chrome BET surface analyzer. The phase composition was characterized using an x-ray diffractometer (XRD) (Phillips X'pert MPD, Cu-K). The crystallite size was calculated by the Scherer equation, equation. (1) [20- 21].

$$D = 0.9\lambda/\beta cos\theta_B \quad (1)$$

Where D is the average crystallite size, k is equal to 0.9, a shape factor for spherical particles, λ is the X-ray wavelength (λ = 0.154

nm), θ is the Bragg angle and $\beta = B - b$, the line broadening. B is the full width of the diffraction line at half of the maximum intensity and b = 0.042 is the instrumental broadening [21].

2.3 Photocatalytic activity test

The photocatalytic activity was evaluated by the degradation of MB under UV irradiation using eleven 50 W of black light lamps. A 10 ml of MB with a concentration of 1×10^{-5} M was mixed with 0.0375 g of powders and kept in a dark chamber for 1 h, after that kept in a chamber under UV irradiation for 0, 1, 2, 3, 4, 5 and 6 h [20]. After photo-treatment for a certain time, the concentration of treated solution was measured by UV-vis spectrometer. The ratio of remained concentration to initial concentration of MB calculated by C/C_0 was plotted against irradiation time in order to observe the photocatalytic degradation and the percentage degradation of the MB molecules (%M) was calculated by Eq. 2, [20].

$$M = 100(C_0\text{-}C)/C_0 \quad (2)$$

Where M is the percentage degradation of the MB molecules, C_0 is the concentration of MB aqueous solution at the beginning (1×10^{-5} M) and C is the concentration of MB aqueous solution after exposure to a light source.

2.4 Antibacterial activity test

Antibacterial activity of the synthesized TiO_2 powder against the bacteria *Escherichia coli* (*E.coli*) was studied. Aliquots of 10 ml *E.coli* conidial suspension (10^5 CFU/ml) were mixed with 0.05 g of the powder [20]. The mixture was then exposed to UV irradiation (eleven 50 W of black light lamps) for 0, 20, 40 and 60 min. After that, 0.1 ml of the mixture suspension was sampled and spread on Macconkey Agar plate and incubated at 37°C for 24 h. After incubation, the number of viable colonies of *E.coli* on each Macconkey Agar plate was observed and disinfection efficiency of each test was calculated in comparison with that of the control (N/N_0) [20]. Percentage of bacterial reduction or percentage of killed *E.coli* was calculated according to the following equation, equation. (3) [20]. The antibacterial activities were test at 3 samples for 1 condition and averaged value from the results.

$$E = 100(N_0\text{-}N)/N_0 \quad (3)$$

Where E is the percentage bacterial reduction or percentage of killed *E.coli*, N_0 and N are the average number of live bacterial cells per milliliter in the flask of the initial or control and powders finishing agent or treated fabrics, respectively.

3. Result and discussion

3.1 Powders characterizations

Figure 1 shows XRD patterns of the TiO_2 powder refluxed at 180 W for various periods of time. The peak locations and relative intensities for TiO_2 were cited from the Joint Committee on Powder Diffraction Standards (JCPDS) database. It was found that only anatase phase was seen for all samples; the peaks locating at 25.40°, 37.8°, 48.00° and 54.15° corresponded to the (101), (004), (200), (105) and (211) planes (JDPDS 21-1272) [22]. The crystallite sizes of nanocrystalline anatase TiO_2 powder that refluxed for 1, 2 and 3 h were found to be about 20.7, 13.8 and 9.3 nm, respectively, which seemed to decrease with an increase in refluxed time due to the contribution of the power from the refluxed time [18].

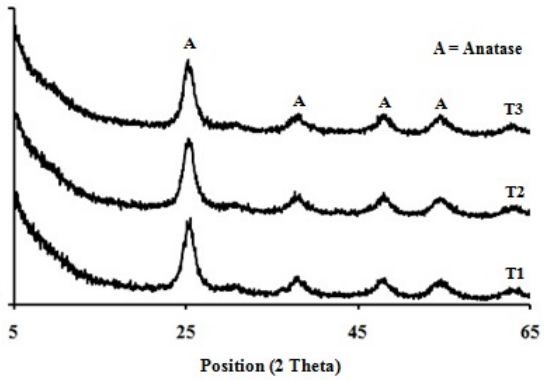

Figure 1 XRD patterns of TiO_2 powder

Figure 2 displays SEM images of the synthesized TiO_2 powder at different hours of the refluxed time. The results revealed that T1, T2 and T3 powders were spherical nanoparticles but agglomerated. As compared to T1, reduction in particle size was obviously observed in T3, suggesting particle size reduction with increasing of the refluxed time. The specific surface areas of T1, T2 and T3 powders were 17.78, 20.17 and 23.48 m^2/g, respectively. The results revealed a significant effect of refluxed time on the crystallite size and specific surface area of the synthesized TiO_2 powder that the 3 h refluxed time (T3) induced the synthesized powder to possess the smallest crystallite size and so the largest specific surface area.

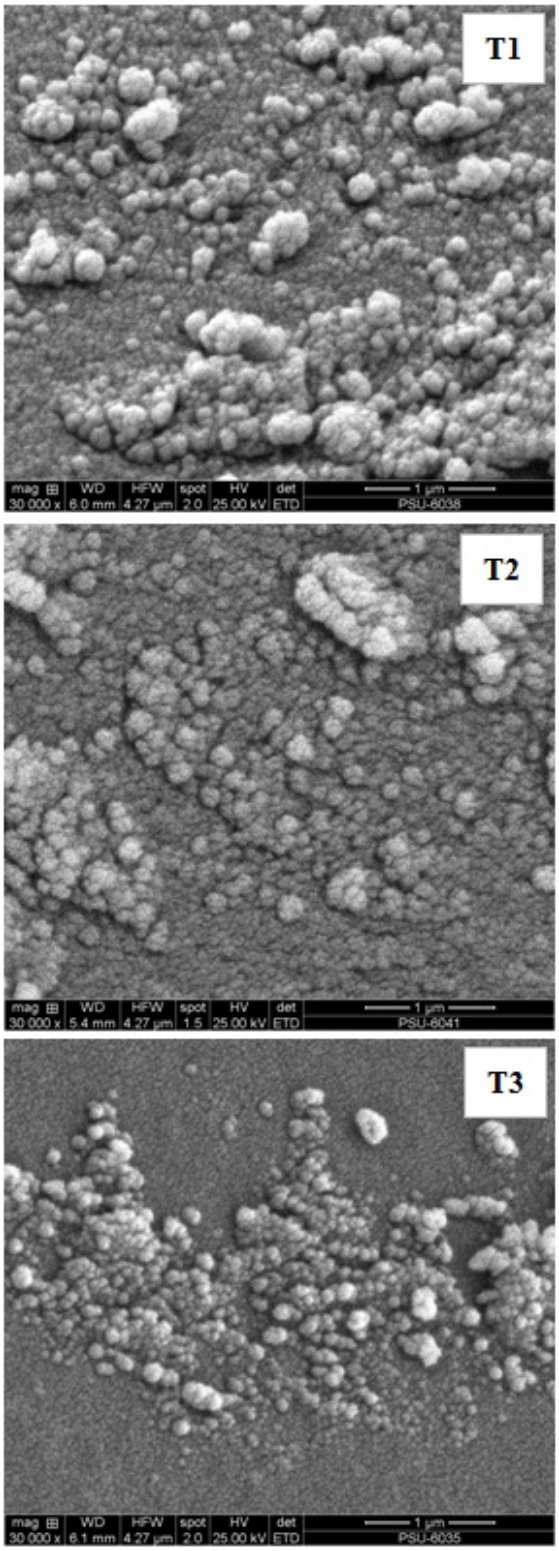

Figure 2 SEM images of surface and morphology of the synthesized TiO_2 powder (magnification 30,000X)

3.2 Photocatalytic activity

Figure 3 illustrates photocatalytic activity of the synthesized TiO_2 powder in methylene blue (MB) solution under UV irradiation for 0, 1, 2, 3, 4, 5 and 6 h. It was found that the photocatalytic activity of TiO_2 powder increased with refluxed time, and thus T3 offered the highest photocatalytic activity. Figure 4 shows the percentage of MB degradation under the light source. After 6 h-UV irradiation, the MB degradation percentage of T3 was 68.66%, while that of T1 and T2 were 50.65 and 59.20%, respectively. Again, the results indicate a great influence of refluxed time on photocatalytic behavior and MB degradation rate of the synthesized powder that the longer refluxed time the better photocatalytic activity.

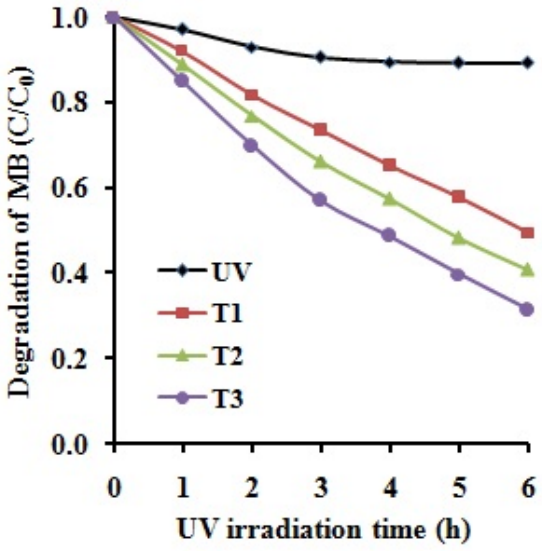

Figure 3 The photocatalytic activity of TiO_2 powder under UV irradiation

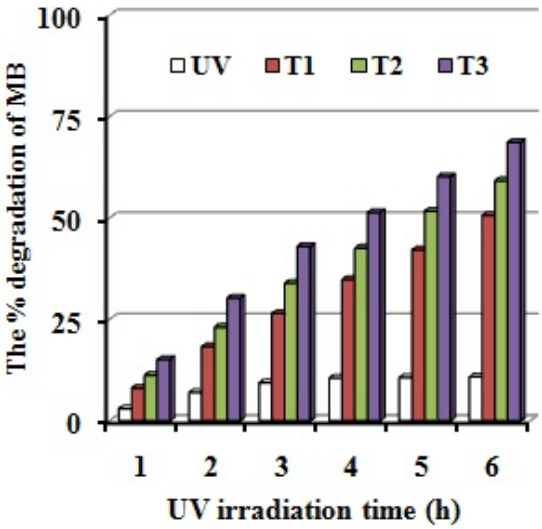

Figure 4 The MB degradation percentage of TiO_2 powder under UV irradiation

3.3 Antibacterial activity

Figure 5 displays the *E.coli* survival rate (N/N_0) after UV illumination on the synthesized TiO_2 powder. The results showed that the *E.coli* survival decreased with irradiation time and hence the highest antibacterial activity was found on T3. Figure 6 demonstrates the percentage of killed *E.coli* of the TiO_2 powder under UV light. The percentage of killed *E.coli* of T1, T2 and T3 were 76.67, 99.33 and 100.00%, respectively, under 1 h-UV irradiation. On the other hand, in the case of testing without TiO_2, the percentage of killed *E.coli* was only 5.00% under 1 h-UV irradiation. **Figure 7** shows an image of the *E.coli* cell wall and membrane damages of TiO_2 powder refluxed for 3 h treated under UV irradiation for 1 h.

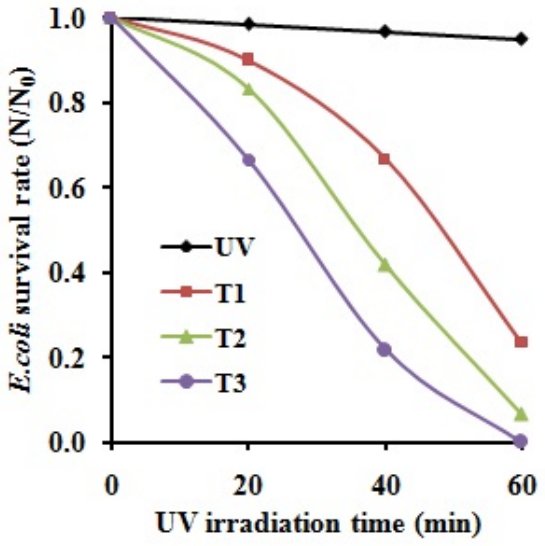

Figure 5 The antibacterial activity of TiO_2 powder under UV irradiation

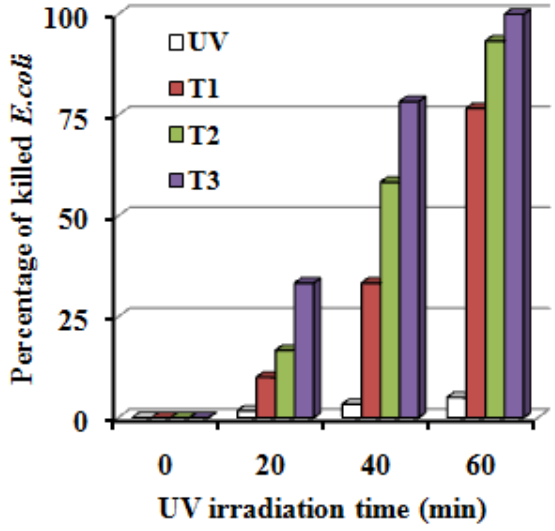

Figure 6 The percentage of killed *E.coli* of TiO_2 powder under UV irradiation

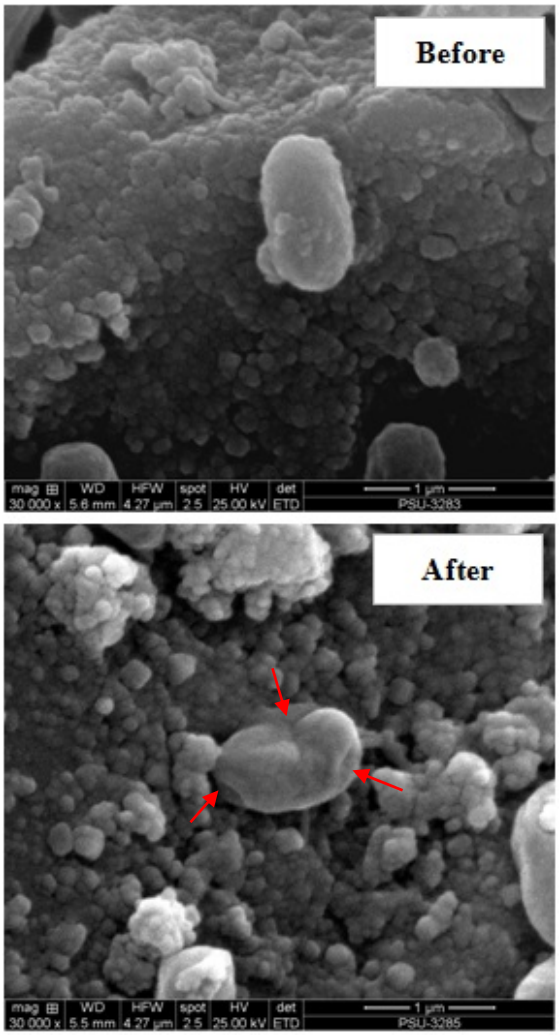

Figure 7 SEM image of the *E.coli* cell wall and membrane damages of TiO_2 powder before and after treated with UV irradiation for 1 h (magnification 30,000X)

Figure 8 illustrates the photograph of viable bacterial colonies (red spots) under UV light of the TiO_2 powder refluxed for 1-3 h in comparison with the control condition (without TiO_2). The results are in good agreement with those presented in Figure 6 that the *E.coli* killing rate increased significantly with refluxed time. The killing efficiency, however, became very poor when TiO_2 was non-existent. This confirms the fact that the synthesized TiO_2 is essential for increasing the *E.coli* killing rate under UV light.

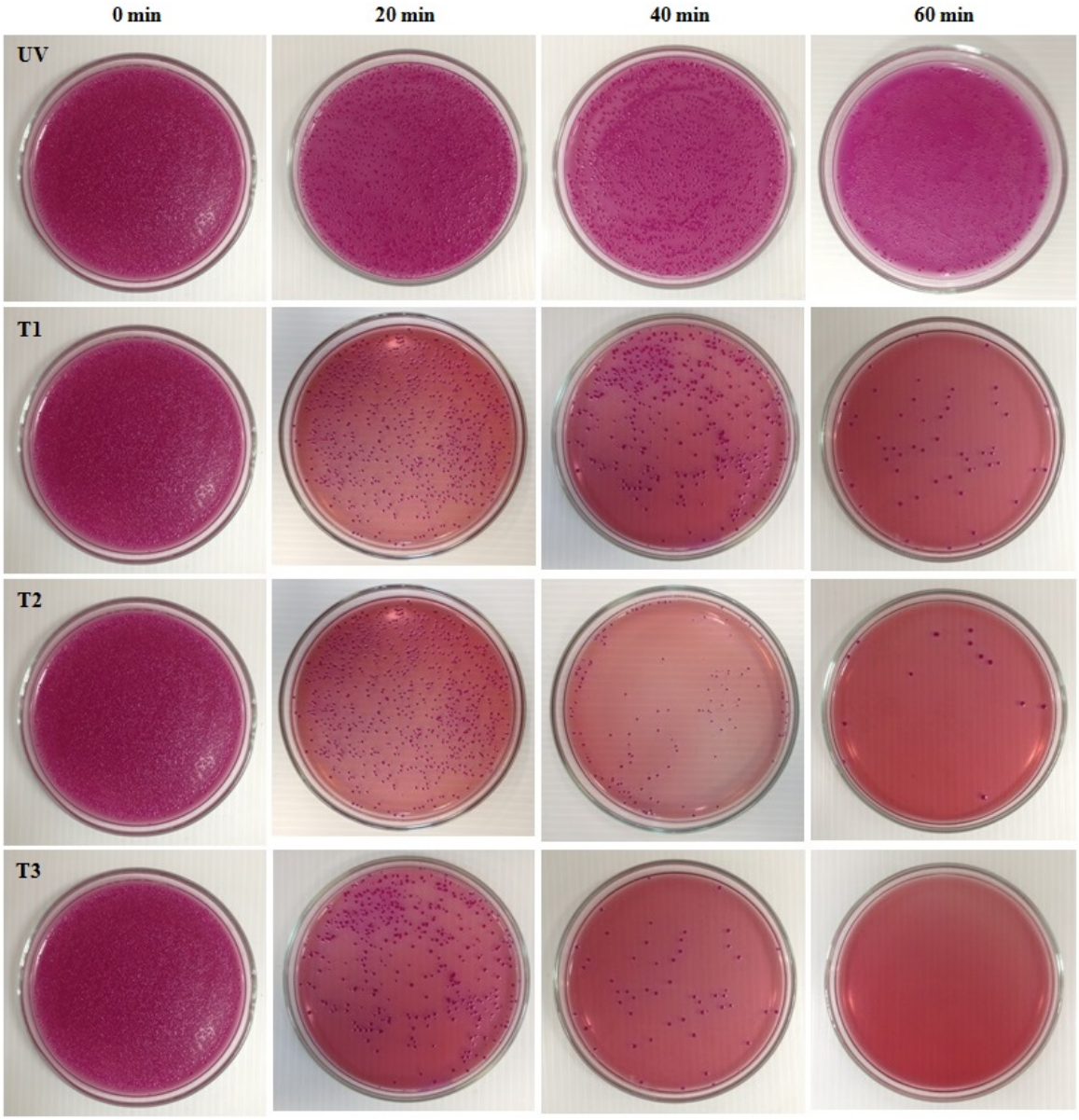

Figure 8 Photograph of viable *E.coli* colonies under UV irradiation of TiO_2 powder compared with control condition (UV case)

4. Conclusions

In this work, TiO_2 powder was fabricated via microwave-assisted sol-gel method which the powder was refluxed at 180 W for 1-3 h and dried at 180 W for 1 h by a conventional microwave oven. The effects of refluxed time on microstructure, photocatalytic and antibacterial activities were investigated and concluded as followings,

1. Nanocrystalline anatase TiO_2 particles with spherical shape were obtained and their crystallite sizes decreased considerably with increasing refluxed time.

2. Photocatalytic and antibacterial activities of the synthesized powder were greatly enhanced when longer refluxed time was applied, and thus the TiO_2 powder refluxed for 3 h offered the highest photocatalytic and antibacterial

activities under UV irradiation with MB degradation percentage of 68.66% and percentage of killed *E.coli* of 100.00%.

3. The presence of anatase TiO_2 was believed to be responsible for such a high efficiency in the photocatalytic and antibacterial activities under UV light.

5. Acknowledgements

The authors would like to acknowledge Institute of Research & Development, Songkhla Rajabhat University and Faculty of Industrial Technology, Songkhla Rajabhat University, Thailand for financial support of this research.

6. Reference

[1] A. Fujishima, T. N. Rao and D. A. Tryk, “Titanium dioxide photocatalysis,” *J. Photoch. Photobio. C*, vol. 1, pp. 1-21, 2000.

[2] G. Mechael, “Dye-sensitized solar cells,” *J. Photoch. Photobio. C*, vol. 4, pp. 145-153, 2003.

[3] M. Gohin, E. Allain, N. Chemin and I. Maurin, “Sol-gel nanoparticulate mesoporous films with enhanced self-cleaning properties,” J. *Photoch. Photobio. A*, vol. 216, pp. 142-148, 2010.

[4] M. S. Hegde, K. Nagaveni and S. Roy, “Synthesis, structure and photocatalytic activity of nano TiO_2 and nano $Ti_{1-x}M_xO_{2-\delta}$ (M = Cu, Fe, Pt, Pd, V, W, Ce, Zr),” *Pramana-J. Phys.*, vol. 46(4), pp. 641-645, 2005.

[5] M. Stamate and G. L. Rom, “Application of titanium dioxide photocatalysis to create self-cleaning materials,” *Rom. Tech. Sci. Aca*., vol. 2, pp. 280-285, 2007.

[6] A. Julian, H. Rengifo, P. Katarzyna and S. Andrzej, “Synthesis, characterization, and photocatalytic cctivities of nanoparticulate N, S-codoped TiO_2 having different surface-to-volume ratios,” *J. Phys. Chem. C*., vol. 114, pp. 2717-2723, 2010.

[7] M. Lazzeri, A. Vittadini and A Selloni, “Structure and energetics of stoichiometric TiO_2 anatase surfaces,” *Phys. Rev. B*., vol. 63, pp. 155409:1-155409:9, 2001.

[8] D. Reyes-Coronada, G. Rodriguez-Gattorno, M. E. Espinosa-Pesqueira, C. Cab, R. Coss and G. Oskam, “Phase-pure TiO_2 nanoparticles: anatase, brookite and rutile,” *Nanotech*., vol. 19(14), pp. 145605:1-145605:10, 2008.

[9] E. Akbar and E. Ameneh, “Effect of crystal structure on photoinduced superhydrophilicity of copper grafted TiO_2 nanostructure thin film,” *Bull. Mater. Sci*., vol. 36(1), pp. 59-63, 2013.

[10] S. J. Tsai and S. Cheng, “Effect of TiO_2: crystalline structure in photocatalytic degradation of phenolic contaminants,” *Catal. Today*, vol. 33, pp. 227-237, 1997.

[11] A. D. Paola, M. Bellardita and L. Plamisano, “Brookite, the least known TiO_2 photocatalyst,” *Catal*., vol. 3, pp. 36-73, 2013.

[12] M. B. Suwarnkar, R. S. Dhabbe, A. N. Kadam and K. M. Garadkar, “Enhanced photocatalytic activity of Ag doped TiO_2 nanoparticles synthesized by a microwave assisted method,” *Cera. Inter*., vol. 40, pp. 5489-5496, 2014.

[13] H. Yang, X. Zhang, Q. Tao and A.Tang, “Microwave-assisted sol-gel synthesis and optical property of TiO_2 thin film,” *J. Optoelectro. Adv. Mater.*, vol. 9(8), pp. 2493-2497, 2007.

[14] B. Zielinska, E. Borowiak-Palen and R. J. Kalenczuk, “A study on the synthesis, characterization and photocatalytic activity of TiO_2 derived nanostructures,” *Mater. Sci. Pol.*, vol. 28(3), pp. 625-367, 2010.

[15] C. S. Kim, B. K. Moon, J. H. Park, S. T. Chung and S. M. Son, “Synthesis of nanocrystalline TiO_2 in toluene by a solvothermal route,” *J. Cryst. Grow.*, vol. 254(3-4), pp. 405-410, 2003.

[16] A. Lagashetty, V, Havanoor, S. Basavaraja, S. D. Balaji and A. Venkatarman, “Microwave-assisted route for synthesis of nanosized metal oxides,” *Sci. Technol. Adv. Mater.*, vol. 8(6), pp. 484-493, 2007.

[17] C. Bandas, C. Lazau, A. Dabici, P. Sfirloaga, N. Vaszilcsin, I. Grozescu and V. Tiponut, “Microwave-assisted hydrothermal method for synthesis of nanocrystalline anatase TiO_2,” *Chem. Bull. “POLITEHNICA” Univ.*, vol. 56(70), pp. 81-84, 2011.

[18] S. Boonyod, W. Sutthisripok and L. Sikong, “Antibacterial activity of TiO_2 and Fe^{3+} doped TiO_2 nanoparticles synthesized at low temperature,” *Adv. Mater. Res.*, vol. 214, pp. 197-201, 2011.

[19] W. Sangchay and T. Rattanakool, “The efficiency of photocatalytic reaction in degradation methylene blue of TiO_2 powders prepared by microwave-assisted sol-gel method,” *Engng. J. CMU.*, vol. 22(1), pp. 18-26, 2015.

[20] W. Sangchay, “Photocatalytic and antibacterial activity of Ag-doped TiO_2 nanoparticles,” *KKU Res. J.*, vol. 18(5), pp. 731-738, 2013.

[21] C. H. Wen, C. C. Yu, C. Hisn and K. T. Ting, “Synthesis and characterization of TiO_2 and Fe/TiO_2 nanoparticles and their performance for photocatalytic degradation of 1, 2-dichloroethane,” *Appl. Sur. Sci.*, vol. 225, pp. 2205-2213, 2008.

[22] S. Dai, Y. Wu, T. Sakai, Z. Du, H. Sakai and M. Abe, “Preparation of highly crystalline TiO_2 nanostructures by acid-assisted hydrothermal treatment of hexagonal-structured nanocrystalline titania/cetyltrimethyammonium bromide nanoskeleton nanoscale,” *Res. Lett.*, vol. 5, pp. 1829-1835, 2010.